JCE

Journal of Civil Engineering
ISSN 2086 - 1206 E-ISSN 2579 - 9029

Shear Behavior Simulation of Reinforced Concrete Beam Incorporating Glass Fibber-Reinforced Polymer Shear Reinforcement

Rahmat D. Sutrisno[a*], Wahyuniarsih Sutrisno[b], Harun Alrasyid[b], Bambang Piscesa[b], Mudji Irmawan[b]

Correspondence

[a]Department of Civil Engineering, Muhammadiyah Gresik University, Gresik, 61121, Indonesia.

[b] Department of Civil Engineering, Institut Teknologi Sepuluh Nopember, Surabaya, 60111, Indonesia.

Corresponding author email adress: rahmatdwisutrisno@umg.ac.id.

Submitted : 29 June 2024
Revised : 15 November 2024
Accepted : 18 November 2024

Abstract

This paper presents the shear behavior of concrete beams incorporating glass fiber-reinforced polymer (GFRP) stirrups using a nonlinear finite element simulation package, 3D-NLFEA. The experimental data was adopted from the test results performed by previous researchers. The constitutive model for the concrete material used in this simulation is based on the plasticity-fracture model and considers the tension-stiffening effect of the concrete. The numerical simulation result was compared with the experimental test, including the ultimate shear force-deflection response and cracking pattern. Based on the analysis result, it was found that the ultimate shear force-deflection response shows almost the same. For the mean ratio of prediction ultimate shear load to actual ultimate shear load from the experimental result and a coefficient of variation of 1.000 and 0.206%, respectively, and deformation results, the mean ratio of prediction deformations for the mid-shear span and mid-span of 0.966 and 0.941, respectively, with the coefficient of variation for the mid shear span and mid-span of 11.849% and 7.627%, respectively. However, the cracking pattern mode of the beam shows good results, which complies with the experimental test.

Keywords:

Shear failure, GFRP, nonlinear finite element, 3D-NLFEA

INTRODUCTION

Corrosion in steel reinforcement is still the main problem in reinforced concrete structures. The influence of extreme weather and environmental conditions that contain a lot of salt and sulphate, such as the marine environment, can accelerate the corrosion process in reinforced steel. This condition causes the need to improve the reinforced concrete structure, so reinforcing materials can withstand corrosion. One of the materials currently being developed to overcome the problem of corrosion in steel reinforcement is noncorrosive FRP reinforcement. According to researchers [1], noncorrosive FRP reinforcement can eliminate the potential of corrosion and the associated deterioration. The use of fiber-reinforced polymer (FRP) composite material in reinforced concrete structures is increasingly used where this material can overcome the main problem with conventional steel reinforcement, especially corrosion. FRP possesses unique mechanical properties, including high tensile strength and corrosion resistance, making it an attractive alternative to traditional steel reinforcement.

Research on FRP reinforcement to replace ordinary steel reinforcement has been conducted by several researchers. Several researchers conducted experiments on the investigation of the behavior of reinforced concrete beams and slab incorporating FRP reinforcement [1], [2], [3]. Research performed by [2] shows that the deflection behavior before the yielding of the beam using glass and carbon FRP is similar to beams with conventional steel reinforcement. However, the beam using FRP bars exhibits higher load-carrying capacity compared to the control sample which uses conventional steel reinforcement.

Furthermore, the shear behavior of FRP-reinforced concrete (RC) beams without shear reinforcement [3], [4], [5] has also been studied. El-Sayed et al [5] performed four bending tests for the concrete slender beam with FRP bars as flexural reinforcement. Those beams were cast without stirrups and subjected to monotonic loading. Based on the research result performed by [3], the slender beam with carbon and glass FRP as flexural reinforcement has a similar behavior to the beam using conventional steel reinforcement. However, the shear strength of concrete beams using FRP bars is not directly proportional to the axial stiffness of the FRP bars, unlike the concrete with conventional steel reinforcement. However, the research results performed by [4] and [5] show that the right amount of FRP reinforcement ratio can increase the shear strength of reinforced concrete beams without shear reinforcement. Other researchers also conducted research related to the shear behavior of concrete members reinforced with FRP stirrup reinforcement [1], [6]. The experimental result performed by [1] shows that GFRP stirrups enhance the concrete contribution after the formation of the first shear crack. The need for efficient shear reinforcement in concrete structures is well-established, as shear failures can

lead to catastrophic consequences. Traditional methods typically involve the use of steel stirrups to enhance shear resistance. However, the advent of advanced materials, such as GFRP, has opened new avenues for improving the shear behavior of concrete elements.

For investigating the response, an experimental test is the most reliable, which can show the real response under the loading. However, the experimental test is often very time-consuming and expensive, so another method is needed to evaluate and predict the behavior of reinforced concrete structures under various loading conditions. In terms of the concrete behavior under loading conditions, the response of reinforced concrete beams can be admitted as linear under normal conditions [7]. The result can be nonlinear when reinforced concrete beams are given a very extreme load, such as a seismic event [8]. The nonlinear response can also occur when the applied load is greater than the capacity of the reinforced concrete beam, such as poor design or construction [9], [10], [11], [12], which for concrete beam structures with FRP reinforcement can also experience the same response. The nonlinear finite element analysis is a technique that can predict the shear capacity of reinforced concrete beams with reasonably accurate results. The nonlinear finite element method and proper concrete constitutive model are necessary to accurately predict peak load and crack patterns associated with concrete shear behavior.

This paper focuses on evaluating the ability of FRP bars to replace conventional steel reinforcement as shear reinforcement in reinforced concrete beam elements with nonlinear finite element analysis. The constitutive beam model used in this study is based on the multi-surface plasticity-fracture model developed by Piscesa et al [13], [14]. The reinforcing bars are modelled as smeared reinforcement rather than embedded formulation, requiring additional explanation in order to calculate the ratio of reinforcement. Precalculating the reinforcement ratio for the input in the modelling would not be feasible for a complex reinforcement system. Researchers Ahmed et al [1] employed the materials for the concrete beam, longitudinal reinforcement, and stirrup reinforcement that are used in this paper.

This paper uses the isotropic fracture model to investigate the shear behavior of reinforced concrete beams. At a certain position in the shear force-deflection curve, the shear force and fracture propagation predictions are shown. The beams with reinforced concrete were modelled as a whole beam. Although some researchers perform simulations with half the beam for symmetrical beams, the cracks that occur can be different between the right and left sides. For the comparison of crack patterns, half of the beam length will be displayed to get the same comparison results as shown by Ahmed et al [1].

RESEARCH SIGNIFICANCE

Several extensive research was performed to study the performance of concrete elements incorporating FRP as the primary reinforcement. However, there was still limited research conducted on the shear behavior of concrete using FRP stirrups, especially the GFRP bars. As durability is one of the most important factors in designing reinforced concrete structures, the study on the use of GFRP bars is crucial to give a deeper understanding of the use of GRFP especially as shear reinforcement. Therefore, this research presents a study on the shear behavior of reinforced concrete beams, including shear capacity, displacement curves, and crack patterns that occur in reinforced concrete beams using an in-house 3D-NLFEA finite element package. In addition, this research also examined the accuracy of the simulation and experimental test of concrete beams incorporating GFRP bars stirrups.

METHODOLOGY

A. CONSTITUTIVE MODEL

The finite element package 3D-NLFEA was developed by [13], [15]. This package uses SALOME as a pre-processor and PARAVIEW as a post-processor [16]. The constitutive model for concrete material used the constitutive model developed by Piscesa et al.[13], [14], [17], and it has been developed by adopting several constitutive models from previous researchers such as [18] and [19]. The constitutive model of Piscesa et al. uses a plasticity-fracture approach, whereas for the failure surface, Piscesa et al. plasticity-fracture using a modified failure surface model from [18] by modifying the parameter which is often used to adjust the peak and residual stress for specific concrete strength, which is known as the frictional driver parameters, based on the equation from [19], [20].

Fracture energy used for concrete beams is calculated based on [21], with a maximum aggregate size set to 25mm. The input for the base fracture energy (GF0) is 0.03 N/mm, where the base tensile fracture energy (GF0) is a function of the maximum aggregate diameter scaled by concrete compressive strength. Furthermore, the tension-stiffening effect is also included in the constitutive model. According to researchers [22], the tension stiffening effect is defined as the ability of the intact concrete between the cracks to withstand part of the tensile forces or the contribution of the intact concrete between the cracks to the stiffness of the structural element. The tension stiffening equation used in the plasticity-fracture model uses an equation based on[23], the equation shown in Equation 1 below.

$$f_{c1} = \frac{f_{cr}}{1+\sqrt{200\,\varepsilon_1}} \quad (1)$$

where f_{c1} is the concrete principal tensile stress, ε_1 is a principal tensile strain in concrete, and f_{cr} is the stress in concrete at cracking. In this model, the tension stiffening is applied directly to all concrete meshes because it affects the concrete's input stress-strain diagram. In this model, tension stiffening is applied directly to entire concrete meshes because it affects the input stress-strain diagram of concrete. During the pre-processor stages, the maximum mesh size of the hexahedral element is set to 25 mm because it adjusts to a predetermined size of maximum aggregate. Hence, theoretically, the internal length scale should be set to 25 mm for reinforced concrete beams.

The constitutive model of the steel reinforcing bar is modelled using an elastic-perfectly plastic model. The material model with the first line as the initial elastic section has the value of the modulus of elasticity of steel, E_s. The second line represents the plasticity of the steel by hardening, and the slope is the hardening modulus, E_{sh}. In

terms of perfect plasticity, where E_{sh} = 0. The limiting strain L indicates the limited ductility of the steel [24].

modulus of elasticity for the steel stirrup were 576 MPa and 200 GPa, respectively.

Table 1 Concrete properties and reinforcement details of test specimens

Test Specimen	Concrete	Flexural Reinforcement			Shear Reinforcement				
	f'_c MPa	Material	f_y MPa	E_s GPa	Material	Diameter mm	Spacing mm	f_{fuv} MPa	E_f GPa
SS-9.5-2	40.8	Nine strand of 15.4 mm diameter seven wire steel strand	1860	200	Steel	9.5	300	f_y = 556	E_s = 200
SG-9.5-2	39.5				GFRP	9.5	300	664	45
SG-9.5-3	41.0				GFRP	9.5	200	664	45
SG-9.5-4	33.5				GFRP	9.5	150	664	45

B. MATERIALS AND BEAM SPECIMENS

In this paper, the material and geometry of the reinforced concrete beam specimens were taken from the experimental test performed by [1]. Researchers [1] tested four large-scale RC beams, including three beams reinforced with GFRP stirrups and one with steel stirrups, which were constructed and tested. The 7.0 m long beams had a T-shaped cross-section measuring a total height of 700 mm, a web width of 180 mm, a flange width of 750 mm, and a flange thickness of 85 mm. The cross-section of the beam can be seen in Figure 1. All four beams using the same longitudinal reinforcement, namely three layers of three 15.4 mm diameter seven-wire steel strands with tensile strength and modulus of elasticity of the seven-wire

According to the test results [1], the GFRP stirrup for the reinforced beam with GFRP stirrup fails at strains reaching an average value of 8890 microstrains. Therefore, in this paper, the simulation of reinforced beams with GFRP stirrups uses the same strain values as described in the study [1], which is expected to get results close to the experimental results carried out by [1]. The concrete properties for all four beams can be seen in Table 1, which also displays the reinforcement properties that will be used for longitudinal reinforcements, GFRP stirrups, and steel stirrups.

The concrete is assumed to have a compressive strength of 0.85f'c, where 0.85 is a factor to reduce the actual concrete strength of the beam to consider the different strength between the concrete beam and the cylinder,

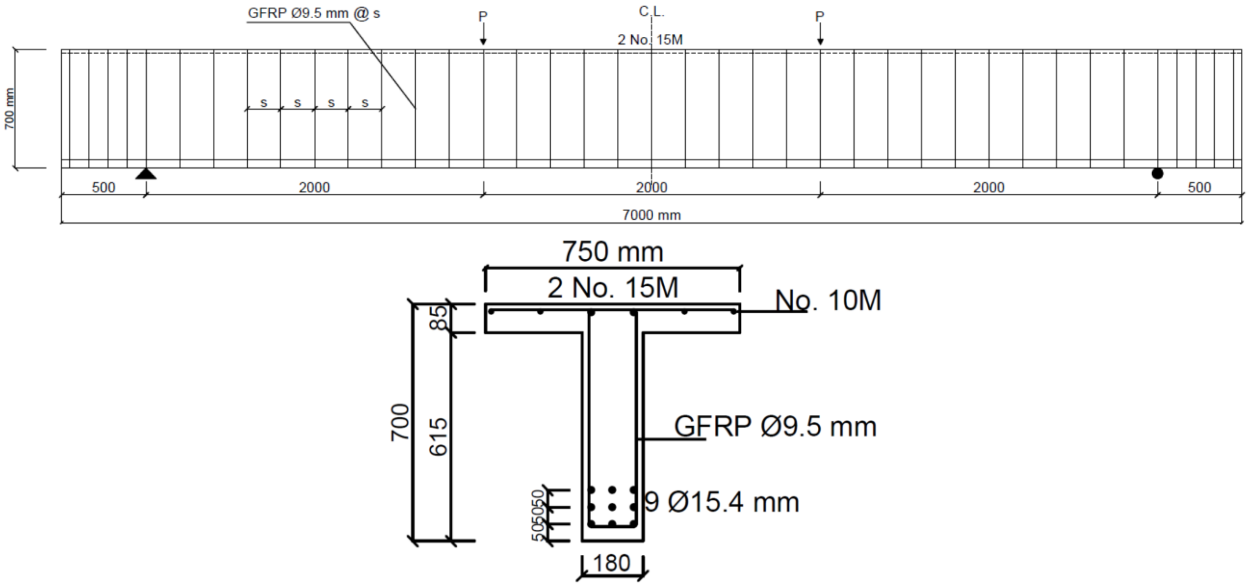

Figure 1 Dimension, Reinforced Details, and Test Scheme of Beam [1]

strands (15.4 mm diameter), were 1860 MPa and 200 GPa, respectively. The transverse reinforcement consisted of 9.5 mm diameter GFRP stirrups for three beams SG-9.5-2, SG-9.5-3, and SG-9.5-4, and 9.5 mm diameter steel stirrups for the fourth beam, SS-9.5-2. The stirrups spacing for the three reinforced beams with GFRP stirrups were 300, 200, and 150 mm. However, stirrup spacing for beams reinforced with steel stirrup was spaced at 300 mm. The yield stress and modulus of elasticity for the GFRP stirrup were 664 MPa and 45 GPa, and the yield stress and

which can be affected by the dimension and curing condition of the specimens. The ACI 318-19 was used to calculate the modulus elasticity for the concrete material. The concrete tensile strength (ft) used as an input takes about 80% of the estimated concrete tensile strength without silica fume, as outlined in [19], [20]. The meshing for beams used an eight-node hexahedral solid element, and the rebar element was simulated using a wire element. Bonding for solid element and wire element using tie constraint type and the boundary condition, which will

define the bearings and loads in the model, using a four-point bending scheme and displacement control loading techniques according to the experimental test conducted by [1]. Figure 1 shows how the beam model is tested. The loading is given with a displacement control of -0.1 mm for every load step.

RESULTS AND DISCUSSIONS

The shear force-deflection output based on the 3D-NLFEA result of four beams is displayed in this section. Table 2 compares the shear force-deflection result between the experimental test and numerical simulation with 3D-NLFEA. According to [1], the test specimens were designed to fail in shear, and the stirrup's strength governed the ultimate shear strength of the test specimens. The ultimate shear force result from the experimental was taken when the stirrup reinforcement in the beam reaches the yield phase for steel stirrups and the rupture phase for GFRP stirrups so that the results of the 3D-NLFEA simulation use the same behavior as the experimental results to get the ultimate shear force.

As shown in Table 2, the ultimate shear force output from the 3D-NLFEA simulation has a similar output as the experimental test with the ratio of ultimate shear force between the experimental test and 3D-NLFEA having average and coefficient of variation of 1.000 and 0.206%, respectively. These results indicate that the results of the 3D-NLFEA have an excellent ability to predict the ultimate shear force, whereas previously explained that the ultimate shear force from the experimental test results is taken when

Table 2 Evaluation of Experimental Results Compared to 3D-NLFEA

Test Specimen	Shear Force (kN)			Deflection (mm)					
	Vu Test	Vu 3D-NLFEA	Vu Test/Vu 3D-NLFEA	Displ. Test		Displ. 3D-NLFEA		Displ. Test/Displ. 3D-NLFEA	
				Mid-Shear Span	Mid Span	Mid-Shear Span	Mid Span	Mid-Shear Span	Mid Span
SS-9.5-2	272.28	272.91	0.998	25.0	49.8	22.4	49.2	1.115	1.013
SG-9.5-2	258.55	258.00	1.002	26.7	46.7	26.8	47.2	0.995	0.989
SG-9.5-3	336.96	336.94	1.000	29.1	55.6	33.8	61.8	0.862	0.900
SG-9.5-4	415.91	415.11	1.002	36.8	68.4	41.3	79.4	0.892	0.861
		Average	**1.000**				**Average**	**0.976**	**0.941**

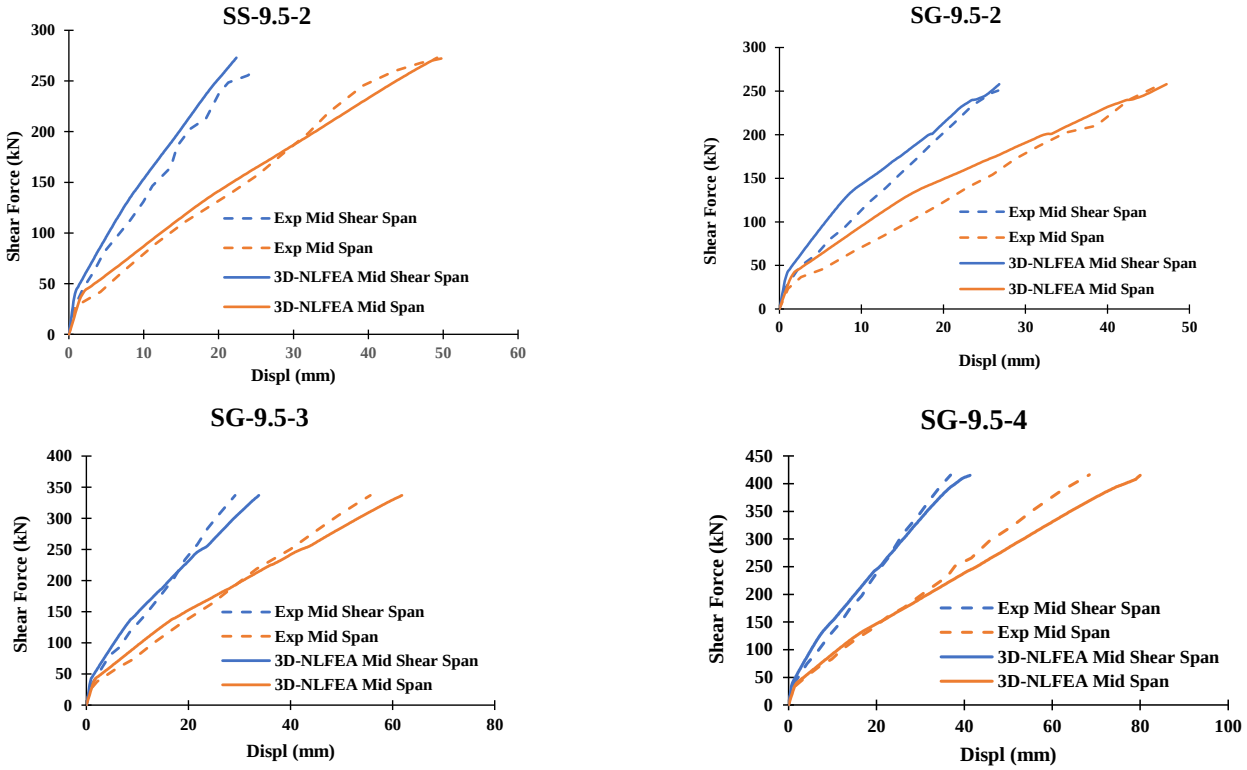

Figure 2 Shear Force and Displacement Comparison Curve [1], Beams with 3D-NLFEA

the reinforcement reaches the yield phase on the steel stirrup and the rupture phase on the GFRP stirrup.

Figure 2 shows the comparison of the shear force-deflection curve for four beams. The deflection from 3D-NLFEA results is slightly different from the experimental results. For beam SS-9.5-2, the displacement ratio between the experimental and the 3D-NLFEA results has values for the displacement ratio at mid-shear and mid-span of 1.115 and 1.013, respectively. These results indicate that the displacement from 3D-NLFEA has a slightly underestimated result compared to the experimental test. For beam SG-9.5-2, the displacement ratio between the experimental results and the 3D-NLFEA results has values for the mid-shear and mid-span of 0.995 and 0.998, respectively. These results indicate that the displacement results from 3D-NLFEA have the same results as the displacement results of the experimental test. For beam SG-9.5-3, the displacement ratio between the experimental and 3D-NLFEA results has values for the mid-shear and mid-span of 0.862 and 0.900, respectively. These results indicate that the displacement results from 3D-NLFEA are slightly overestimated compared to the displacement results of the experimental test. For beam SG-9.5-4, the displacement ratio between the experimental and 3D-NLFEA results has values for the mid-shear and mid-span of 0.892 and 0.861, respectively. These results indicate that the displacement results from 3D-NLFEA are slightly overestimated compared to the displacement results of the experimental test.

On the other hand, for the combination of the four beams, the displacement comparison between the experimental results and the 3D-NLFEA results has an average ratio for the mid-shear span and mid-span of 0.976 and 0.941, respectively, with the coefficient of variation for the mid shear span and mid-span of 11.849% and 7.627%. These results show that overall, the 3D-NLFEA results have slightly overestimated results from the mid-shear and mid-span displacements for four beams. This could be caused by the addition of a tension-stiffening effect, which, according to [22] the tension stiffening effect is expressed as the contribution of the intact concrete between the cracks to the stiffness of the structural elements or the ability of the intact concrete between the cracks to withstand some of the resulting tensile forces. In this model, the tension stiffening effect was considered, resulting in increased shear and flexural strength of the reinforced concrete beam. The cracked concrete's contribution also increases the beam's nonlinear stiffness under stress. All those effects were combined and finally caused an increase in the displacement of the beam [22].

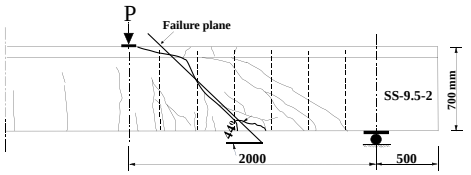

SS-9.5-2 Experimental

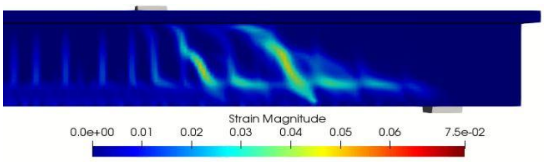

SS-9.5-2 3DNLFEA

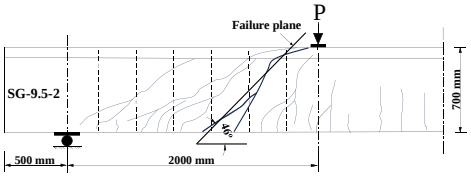

SG-9.5-2 Experimental

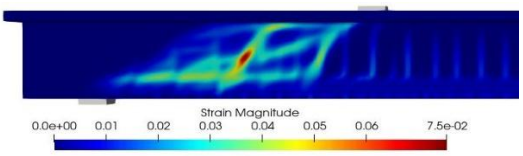

SG-9.5-2 3DNLFEA

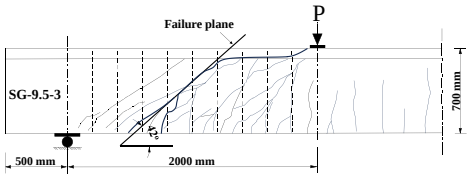

SG-9.5-3 Experimental

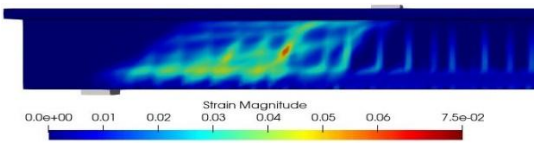

SG-9.5-3 3DNLFEA

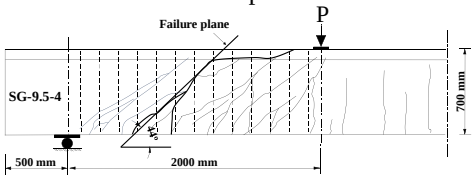

SG-9.5-4 Experimental

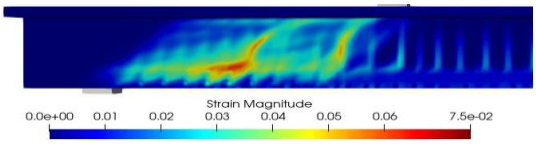

SG.9.5-4 3DNLFEA

Figure 3 Crack Pattern Comparison for Ahmed et al. [1] beams with 3DNLFEA

A comparison of the crack patterns between the 3D-NLFEA numerical simulation analysis and the experimental results can be seen in Figure 3, where the comparison of the crack patterns that occur in the beam's

half span is in accordance with the results shown in the study [1].

As shown in Figure 3, the crack pattern of the 3DNLFEA results is the same as that of the experimental results. Researchers [1] stated that the crack pattern that occurs in the beam is described as shear compression in the Shear Span region, and in the mid-span region, it is described as flexural compression. The same thing happened in the 3D-NLFEA model where, in the Shear Span area, the crack pattern that occurs in the beam is described as shear compression, and in the mid-span area, it is described as flexural compression, so these results show that the 3DNLFEA auxiliary program can predict the beam crack pattern well according to with experimental results.

CONCLUSIONS

This paper aims to evaluate the shear behavior of glass fiber reinforced polymer stirrup for reinforced concrete beams using nonlinear finite element simulation. The concrete constitutive model used the plasticity fracture model and tension stiffening effect. The 3D-NLFEA software package was used in the numerical simulation to utilize a full three-dimensional model of the beam and random imperfection material to get results for nonlinear finite element simulation.

Based on the result, the plasticity fracture model and tension stiffening effect can provide acceptable shear force and deflection predictions for reinforced concrete beams. The mean shear force of experimental to 3D-NLFEA (Vu Test/Vu 3D-NLFEA) has a ratio of 1.000 and a coefficient of variation of 0.206%. These results indicate that the 3D-NLFEA has a good ability to predict the ultimate shear force. On the other hand, the displacement ratio of experimental and 3D-NLFEA has an average ratio of 0.976 and 0.941 for the mid-shear span and mid-span, respectively. The coefficient of variation for the mid shear span and mid-span are 11.849% and 7.627%, respectively.

For crack pattern comparison, the result from 3D-NLFEA is similar with the experimental result. In the experimental result, the crack pattern that occurs in the beam is described as shear compression in the shear span region, and in the mid-span region, it is described as flexural compression. The same thing happened in the 3D-NLFEA model where, in the shear span area, the crack pattern that occurs in the beam is described as shear compression, and in the mid-span area, it is described as flexural compression.

The results show that the 3D-NLFEA software package can produce results that are close to the experimental results, which can help engineers assess and predict the response of structural elements in detail. Post-processing in 3D-NLFEA can be very helpful in the process of predicting a structural element as well as assessing its ability.

REFERENCES

[1] E. A. Ahmed, E. F. El-Salakawy, and B. Benmokrane, "Performance evaluation of glass fiber-reinforced polymer shear reinforcement for concrete beams," *ACI Struct. J.*, vol. 107, no. 6, pp. 738–740, 2010.

[2] E. El-Salakawy and B. Benmokrane, "Serviceability of concrete bridge deck slabs reinforced with fiber-reinforced polymer composite bars," *ACI Struct. J.*, vol. 101, no. 5, pp. 727–736, 2004, doi: 10.14359/13395.

[3] B. Benmokrane, O. Chaallal, and R. Masmoudi, "Flexural response of concrete beams reinforced with FRP reinforcing bars," *ACI Struct. J.*, vol. 93, no. 1, pp. 46–55, 1996, doi: 10.14359/9839.

[4] G. Markou and M. Alhamaydeh, "3D Finite Element Modeling of GFRP-Reinforced Concrete Deep Beams without Shear Reinforcement," *Int. J. Comput. Methods*, vol. 15, no. 2, pp. 1–35, 2018, doi: 10.1142/S0219876218500019.

[5] A. K. El-Sayed, E. F. El-Salakawy, B. Benmokrane, E. G. Sherwood, E. C. Bentz, and M. P. Collins, "Shear strength of FRP-reinforced concrete beams without transverse reinforcement," *ACI Struct. J.*, vol. 104, no. 1, pp. 113–114, 2007.

[6] H. Kim, M. S. Kim, M. J. Ko, and Y. H. Lee, "Shear Behavior of Concrete Beams Reinforced with GFRP Shear Reinforcement," *Int. J. Polym. Sci.*, vol. 2015, 2015, doi: 10.1155/2015/213583.

[7] A. Tambusay, P. Suprobo, B. Suryanto, and W. Don, "Application of nonlinear finite element analysis on shear-critical reinforced concrete beams," *J. Eng. Technol. Sci.*, vol. 53, no. 4, 2021, doi: 10.5614/j.eng.technol.sci.2021.53.4.8.

[8] B. Il Bae, J. H. Chung, H. K. Choi, H. S. Jung, and C. S. Choi, "Experimental study on the cyclic behavior of steel fiber reinforced high strength concrete columns and evaluation of shear strength," *Eng. Struct.*, vol. 157, no. December 2017, pp. 250–267, 2018, doi: 10.1016/j.engstruct.2017.11.072.

[9] M. M. Ziara, D. Haldane, and S. Hood, "Proposed changes to flexural design in BS 8110 to allow over-reinforced sections to fail in a ductile manner," *Mag. Concr. Res.*, vol. 52, no. 6, pp. 443–454, 2000, doi: 10.1680/macr.2000.52.6.443.

[10] A. Sharma, R. Eligehausen, and J. Hofmann, "Seismic Assesment of Poorly Designed RC Frame Structures Seismic Assesment of Poorly Designed RC Frame Structures Considering Joint," no. November, 2014, doi: 10.13140/2.1.2516.9608.

[11] K. V. Duong, S. A. Sheikh, and F. J. Vecchio, "Seismic behavior of shear-critical reinforced concrete frame: Experimental investigation," *ACI Struct. J.*, vol. 104, no. 3, pp. 304–313, 2007, doi: 10.14359/18620.

[12] M. P. Collins, E. C. Bentz, E. G. Sherwood, and J. K. Wight, "Where is shear reinforcement required? review of research results and design procedures.," *ACI Struct. J.*, vol. 106, no. 4, p. 556, 2009.

[13] B. Piscesa, M. M. Attard, D. Prasetya, and A. K. Samani, "Modeling cover spalling behavior in high strength reinforced concrete columns using a plasticity-fracture model," *Eng. Struct.*, vol. 196, no. June, p. 109336, 2019, doi: 10.1016/j.engstruct.2019.109336.

[14] B. Piscesa, H. Alrasyid, D. Prasetya, and D. Iranata, "Numerical Investigation of Reinforced Concrete Beam Due to Shear Failure," *IPTEK J.*

Technol. Sci., vol. 31, no. 3, p. 373, 2021, doi: 10.12962/j20882033.v31i3.7385.

[15] B. Piscesa, M. M. Attard, and A. K. Samani, "3D Finite element modeling of circular reinforced concrete columns confined with FRP using a plasticity based formulation," *Compos. Struct.*, vol. 194, pp. 478–493, 2018, doi: 10.1016/j.compstruct.2018.04.039.

[16] U. Ayachit, "The ParaView Guide: A Parallel Visualization Application," 2015.

[17] B. Piscesa, M. M. Attard, and A. K. Samani, "A lateral strain plasticity model for FRP confined concrete," *Compos. Struct.*, vol. 158, pp. 160–174, 2016, doi: 10.1016/j.compstruct.2016.09.028.

[18] P. Menetrey and K. J. Willam, "Triaxial Failure Criterion for Concrete and Its Generalization," no. 92, pp. 311–318, 1996.

[19] M. M. Attard and S. Setunge, "Stress-strain relationship of confined and unconfined concrete," *ACI Mater. J.*, vol. 93, no. 5, pp. 432–442, 1996, doi: 10.14359/9847.

[20] A. K. Samani and M. M. Attard, "A stress-strain model for uniaxial and confined concrete under compression," *Eng. Struct.*, vol. 41, pp. 335–349, 2012, doi: 10.1016/j.engstruct.2012.03.027.

[21] CEB-FIP, "CEB FIP model code 1990." p. 462, 1990.

[22] M. P. Martins, C. S. Rangel, M. Amario, J. M. F. Lima, P. R. L. Lima, and R. D. Toledo Filho, "Modelling of tension stiffening effect in reinforced recycled concrete," *Rev. IBRACON Estruturas e Mater.*, vol. 13, no. 6, pp. 1–21, 2020, doi: 10.1590/s1983-41952020000600005.

[23] F. J. Vecchio and M. P. Collins, "Modified Compression-Field Theory for Reinforced Concrete Elements Subjected To Shear.," *Journal of the American Concrete Institute*, vol. 83, no. 2. pp. 219–231, 1986. doi: 10.14359/10416.

[24] V. Červenka and J. Červenka, "Atena Theory Updated," pp. 1–33, 2018.